

blood

Prepublished online Jun 3, 2008;
doi:10.1182/blood-2008-04-149773

The membrane-bound serine protease matriptase-2 (Tmprss6) is an essential regulator of iron homeostasis

Alicia R Folgueras, Fernando Martin de Lara, Alberto M Pendas, Cecilia Garabaya, Francisco Rodriguez, Aurora Astudillo, Teresa Bernal, Ruben Cabanillas, Carlos Lopez-Otin and Gloria Velasco

Information about reproducing this article in parts or in its entirety may be found online at:
http://bloodjournal.hematologylibrary.org/misc/rights.dtl#repub_requests

Information about ordering reprints may be found online at:
<http://bloodjournal.hematologylibrary.org/misc/rights.dtl#reprints>

Information about subscriptions and ASH membership may be found online at:
<http://bloodjournal.hematologylibrary.org/subscriptions/index.dtl>



The membrane-bound serine protease matriptase-2 (Tmprss6) is an essential regulator of iron homeostasis

Alicia R. Folgueras¹, Fernando Martín de Lara¹, Alberto M. Pendás¹,
Cecilia Garabaya¹, Francisco Rodríguez¹, Aurora Astudillo², Teresa
Bernal³, Rubén Cabanillas⁴, Carlos López-Otín¹, and Gloria Velasco¹

*From the Departamento de Bioquímica y Biología Molecular¹, Facultad de Medicina,
Instituto Universitario de Oncología, Universidad de Oviedo, 33006-Oviedo, Spain;
and Servicio de Anatomía Patológica², Hematología³ and Otorrinolaringología⁴,
Hospital Universitario Central de Asturias, 33006-Oviedo, Spain*

A.M.P. present address: Centro de Investigación del Cáncer, CSIC-Universidad de
Salamanca, Salamanca-Spain.

Running title: Matriptase-2 regulates iron metabolism

Send correspondence to:

Carlos Lopez-Otin
Departamento de Bioquímica y Biología Molecular
Facultad de Medicina, Universidad de Oviedo
33006 Oviedo, Spain
Tel. 34-985-104201; Fax: 34-985-103564
E-mail: clo@uniovi.es

Abstract

Proteolytic events at the cell surface are essential in the regulation of signal transduction pathways. Over the last years, the family of type II transmembrane serine proteases (TTSPs) has acquired an increasing relevance due to their privileged localization at the cell surface, although our current understanding of the biological function of most TTSPs is very limited. Here we demonstrate that matriptase-2 (*Tmprss6*), a recently described member of the TTSP family, is an essential regulator of iron homeostasis. Thus, *Tmprss6*^{-/-} mice display an overt phenotype of alopecia and a severe iron deficiency anemia. These hematological alterations found in *Tmprss6*^{-/-} mice are accompanied by a marked up-regulation of hepcidin, a negative regulator of iron export into plasma. Likewise, *Tmprss6*^{-/-} mice have reduced ferroportin expression in the basolateral membrane of enterocytes and accumulate iron in these cells. Iron-dextran therapy rescues both alopecia and hematological alterations of *Tmprss6*^{-/-} mice, providing causal evidence that the anemic phenotype of these mutant mice results from the blockade of intestinal iron export into plasma after dietary absorption. Based on these findings, we conclude that matriptase-2 activity represents a novel and relevant step in hepcidin regulation and iron homeostasis.

Introduction

Pericellular proteolysis is an essential event that determines the relationships between the cell and its microenvironment. This crucial process in the development and maintenance of multicellular organisms requires the remodelling of extracellular matrix components as well as the post-translational regulation of a wide range of cell surface receptors, regulatory proteins and adhesion molecules.¹ The increasing relevance of proteolytic processes localized at the cell surface has attracted notable attention on membrane-associated proteolytic systems, including the family of type II transmembrane serine proteases (TTSPs).^{2,3} The TTSP family is composed of more than 20 different members that share a number of structural features: a single-pass transmembrane domain located near the short cytoplasmic amino-terminal tail, a central region containing different protein-interacting domains, and a carboxy-terminal catalytic region with the structural characteristics of serine proteases. The large variability of the central modular region together with the diverse expression patterns of TTSP family members suggest that these enzymes may play different physiological and pathological roles, although only a few of these functions have been identified so far. Thus, enteropeptidase is mainly expressed in the duodenum and plays an essential role in food digestion as activator of pancreatic trypsinogen to trypsin.⁴ Hepsin, is mainly expressed in liver, but is highly up-regulated in prostate cancer.^{5,6} Matriptase/MT-SP1 is a widely studied member of the TTSP family due to its relevance in diverse processes including cancer progression.^{7,8} Mutant mice deficient in matriptase die shortly after birth due to aberrant skin development that compromises epidermal barrier function and causes mice dehydration.⁹ Corin is a TTSP family member mainly expressed in the heart and involved in the activation of pro-atrial natriuretic peptide, a cardiac hormone essential for the regulation of blood pressure.¹⁰ TMPRSS2 and TMPRSS4 are up-regulated or structurally altered in prostate cancer.^{11,12} Other members of this protease family whose physiological and pathological roles still remain unclear are spinesin/TMPRSS5,¹³ MSPL (mosaic serine protease large form),¹⁴ matriptase-3,¹⁵ polyserase-1,¹⁶ as well as the different components of the HAT (human airway trypsin-like protease)/DESC (differentially expressed in squamous cell carcinoma) subfamily.^{17,18}

Matriptase-2 (TMPRSS6) is another TTSP family member of unknown function but whose study has achieved particular interest due to its structural and enzymatic similarities with matriptase and to its putative role as a tumor suppressor enzyme in human breast cancer.¹⁹⁻²¹ This enzyme was first identified and cloned in our laboratory¹⁹ as part of our ongoing studies aimed at characterizing the human degradome, which is defined as the complete set of proteases produced by human cells.^{22,23} Matriptase-2 expression is mainly circumscribed to liver in both human and mouse, suggesting tissue-specific functions for this enzyme.^{19,24} Nevertheless, minor matriptase-2 expression has also been detected in kidney, uterus and the nasal cavity.²⁴ Matriptase-2 shares the structural organization of TTSPs including the short cytoplasmic domain, a type II transmembrane sequence, a stem region with two CUB (complement factor C1s/C1r, urchin embryonic growth factor, bone morphogenetic protein) domains and three LDLR (low density lipoprotein receptor) tandem repeats, and the carboxy-terminal serine protease domain.^{19,24} In addition, matriptase-2 contains a SEA (sea urchin sperm protein, enteropeptidase, agrin) domain which conserves a potential cleavage motif sequence that may release the enzyme from the cell surface, as reported for other TTSPs.²⁰ Matriptase-2 has the ability to degrade *in vitro* extracellular matrix components such as fibronectin, fibrinogen and type I collagen, and to activate single-chain uPA although with low efficiency compared to matriptase.¹⁹ However, at present, very little information is available about the *in vivo* functional relevance of matriptase-2 in both physiological and pathological processes. To further characterize the *in vivo* role of this type II transmembrane serine protease, we have generated mutant mice deficient in matriptase-2. In this work, and after a series of phenotypic and molecular analysis of *Tmprss6*^{-/-} mice, we provide evidence that matriptase-2 is an essential regulator of iron homeostasis.

Material and Methods

Tmprss6 gene targeting

A 3'-*Hprt* chromosomal engineering targeting vector was used to generate *Tmprss6*^{-/-} mice following an insertional targeting strategy.²⁵ A 7,068 bp homology region, containing exons 3 to 6, was PCR-amplified from a murine genomic 129S7-derived PAC clone by using Long-Expand High Fidelity PCR mix (Roche Applied Science) and it was cloned into the *AscI* site of the 3'-*Hprt* vector (a kind gift of Dr. A. Bradley). The targeting vector was digested with *EcoRI* to remove an internal *EcoRI* fragment in the homology region and create a "gap" that will be repaired during the targeting event. The targeting vector was linearized by digestion with *EcoRI* and electroporated into HM1 embryonic stem cells. Resistant clones were selected with puromycin by using standard protocols. Homologous recombination was confirmed in the screened clones by Southern blot hybridization with the gap region which was used as a probe, after *NdeI* digestion. During the targeting event the gap is repaired and, as a consequence of the duplicated region generated, a novel 18 kb fragment is detected by the gap probe in addition to the 9 kb wild-type fragment. The heterozygous stem cells identified were aggregated to CD1 morulas and transferred into uteri of pseudopregnant females to generate chimeras. Chimeric males were mated with C57BL/6J females. A new strategy of genotyping was used to screen the offspring by using Southern blotting analysis of tail genomic DNA digested with *SspI* and hybridized with a 3'-external probe amplified from a genomic PAC. This probe was a 593 bp fragment amplified with primers 5'-GTCTCAGGTTCCCTGAGCCTG-3' and 5'-GTGCCAAACACTCAGGG ATGC-3'.

Northern blot analysis

Total RNA was isolated from frozen liver samples obtained from wild-type and mutant adult mice by using a commercial kit (RNeasy Mini Kit; Qiagen). A total of 10 µg of denatured RNA from liver was separated by electrophoresis on agarose gels and transferred to Hybond N+ (Amersham Pharmacia Biotech). Blots were hybridized with random primed ³²P-labeled cDNA probes for mouse *Tmprss6* and hepcidin. The cDNA probe for hepcidin was obtained by reverse transcription PCR (RT-PCR) using 1 µg of total RNA from mouse liver and oligodT as primer, according to the manufacturer's instructions (Invitrogen). After RT, 2 µl of the mixture were used for PCR with the

following murine hepcidin specific oligonucleotides: mHepcidinFw: 5'-CAGCAGAACAGAAGGCATGA and mHepcidinRv: 5'-AGATGCAGATGGGGAAGTTG. The specific probe used to detect *Tmprss6* was prepared from the murine *Tmprss6* cDNA plasmid by digestion with BamHI. Blots were rehybridized with a β -actin cDNA probe as an indicator of RNA loading.

Transcriptional profiling and real-time quantitative PCR

Total RNA was isolated as described before. Double-stranded cDNA was synthesized using the SuperScript™ cDNA synthesis kit (Invitrogen). *In vitro* transcription was carried out with the Bioarray high yield RNA transcript labeling kit (Enzo Diagnostic). The biotin-labeled cRNA was purified, fragmented, and hybridized to GeneChip Mouse 430 2.0 Array (Affymetrix). Real-time quantification of hepcidin transcript levels was performed by using Applied Biosystems Taqman gene expression assays in an ABI7000 Sequence detection system (Applied Biosystems) following the manufacturer's instructions. Hepcidin transcript abundance was calculated in triplicated relative to the expression of the stable housekeeping gene β -actin. The average relative expression of hepcidin in wild-type mice was assigned an arbitrary value of 100 in each experiment.

Blood analysis and iron-dextran treatment

Mouse experimentation was done according to the guidelines of the University of Oviedo, Oviedo-Spain. Whole blood was collected retro-orbitally into heparinized-coated tubes. Plasma iron and unsaturated iron binding capacity (UIBC) were determined using a colorimetric method (Biolabo, Maizy, France). The total iron binding capacity (TIBC) was calculated as the sum of plasma iron and UIBC, and the percentage of transferrin saturation using the formula plasma iron/TIBC x 100. Peripheral blood smears were stained with Wright-Giemsa stain (Fisher Diagnostics) for morphological examination. Where indicated, 5 mg (8-week-old) or 2 mg (10-day-old) iron-dextran (Sigma) was injected subcutaneously weekly to knock-out mice.

Tissue iron staining and immunohistochemistry

Duodenal samples were fixed in 4% formaldehyde and embedded in paraffin. Deparaffined tissue sections were stained with Perls Prussian blue stain for non-heme iron, following nuclear red counterstaining by using standard procedures. To perform immunohistochemistry analysis, deparaffined and rehydrated sections were rinsed in

PBS (pH 7.5). Sections were incubated overnight at 4 °C with a rabbit polyclonal antibody anti-mouse ferroportin (Lifespan Biosciences), diluted 1:100. Then, sections were incubated with an anti-rabbit EnVision system labelled polymer-HRP (DakoCytomation) for 30 min, washed and visualized with diaminobenzidine. Sections were counterstained with Mayer's hematoxylin, dehydrated and mounted in Entellan®. Sections were examined using a Nikon Eclipse E400 microscope and images were acquired with a Nikon DS-Si1 camera and Nikon NIS-Elements F2.20 software.

Statistical analysis

The mean values and the corresponding standard error of the mean (SEM) were calculated. Differences between mean values were analyzed by two-tailed Student's *t* test. A value of $P < 0.05$ was considered significant. Statistically significant differences are shown with asterisks.

All microarray data has been deposited in Gene Expression Omnibus (GEO) under accession number GSE11632.

Results

Generation of mice deficient in matriptase-2

To analyze the *in vivo* role of matriptase-2, we designed an insertion vector for gene targeting, in order to provide a high targeting frequency²⁵ (Figure 1A). According to this strategy, after electroporation into HM-1 embryonic stem cells (129/Ola background), the linearized and gapped vector would integrate into the target locus generating a duplication of the entire region of homology including the repaired gap sequence (Figure 1B). By following this procedure, we finally identified several correctly targeted clones that were used to generate chimeras and finally heterozygous mice. After intercrossing heterozygous mice from the F1 generation, we obtained *Tmprss6*^{+/+}, *Tmprss6*^{+/-} and *Tmprss6*^{-/-} mice in the expected Mendelian ratios (Figure 1C). Northern blot analysis of total RNA from liver of wild-type and *knock-out* animals confirmed the complete absence of *Tmprss6* transcript in *Tmprss6*^{-/-} mice (Figure 1D). *Tmprss6*^{-/-} mice exhibited slight signs of growth retardation that were more pronounced in female mice. Thus, we observed significant differences between the body weight of 4-week-old control and mutant female mice (control: 12.0 ± 0.4 g, n=26 vs knock-out: 10.2 ± 0.5 g, n=15; P<0.05). Likewise, we observed a marked retardation in ovarian maturation in adult *Tmprss6*^{-/-} females that could be linked to the infertility observed in these mutant females.

Tmprss6^{-/-} mice exhibit a cyclic hair loss phenotype

Mice deficient in *Tmprss6* display an overt phenotype of alopecia. *Knock-out* pups started to show hair loss on the back at approximately two weeks of age, although the head of these mutant mice did not show any evidence of hair loss. By four weeks of age, *Tmprss6*^{-/-} mice displayed a completely nude phenotype in the dorsal and ventral

regions of the thorax and abdomen (Figure 2A). This alopecia condition lasted for approximately ten days and then new hair growth was initiated, as revealed by the change in back skin colour followed by a complete recovery of the hair. A few days later, a progressive hair loss began again and a phenotype of diffuse alopecia in the dorsal region was definitively maintained during adult life. Histological analysis revealed that skin from 4-week-old mice had a reduced number of pillar units and the hair follicles were disorganized, dystrophic and hypoplastic, showing a thinner outer root sheath at the isthmus and inferior segment level. Likewise, mutant mice displayed a pronounced infundibular ectasia with hyperkeratosis (Figure 2B). In adult *Tmprss6*^{-/-} mice, the reduced number of pillar units as well as the hypoplastic phenotype were also observed in the skin. However, the hyperkeratosis and ectasia almost disappeared (data not shown).

Hepcidin up-regulation causes severe anemia in *Tmprss6*^{-/-} mice

The phenotypic features of hair loss present in *Tmprss6*^{-/-} mice, together with the observation of an evident pallor phenotype in newborn mice and the occurrence of several signs of growth retardation and female infertility, prompted us to analyze a series of hematological parameters in blood samples of these mutant mice. Plasma analysis revealed that *Tmprss6*^{-/-} mice were anemic and displayed both a severe iron deficiency and reduced transferrin saturation (Table 1). Likewise, Wright-Giemsa-stained blood smears from *Tmprss6*^{-/-} mice revealed a severe hypochromia and a slight phenotype of anisocytosis and poikilocytosis in comparison to wild-type counterparts (Figure 3A-B). These morphological observations were confirmed after the quantification of several red blood cell parameters (Table 2). Considering this anemic phenotype observed in *Tmprss6*^{-/-} mice and the restricted expression pattern of this protease, which is mainly circumscribed to the liver, we hypothesized that the absence of matriptase-2 (*Tmprss6*) in this essential organ for iron homeostasis might alter certain regulatory factors involved in iron metabolism, alterations which could in turn contribute to explain the observed phenotype. To evaluate this possibility, we used oligonucleotide-based microarrays to analyze transcriptional changes in liver from *Tmprss6*^{-/-} mice. Out of 45,000 gene sequences present in the array, a total of 471 (1.05%) showed a higher than 2.5-fold decrease in expression levels in liver from *Tmprss6*^{-/-} when compared with control mice, whereas 221 genes (0.49%) were up-

regulated more than two-fold (Supplementary Table 1). Analysis of these results revealed that hepcidin, the principal hormonal regulator of systemic iron homeostasis, was clearly up-regulated in *Tmprss6*^{-/-} mice when compared to wild-type animals. Northern blot analysis and qPCR of liver RNAs from different *Tmprss6*^{-/-} mice confirmed that hepcidin was significantly up-regulated (2.5-fold increase) in mice deficient in this serine protease (Figure 3C-D). Additional studies revealed that this hepcidin up-regulation was already present in *Tmprss6*^{-/-} mice since birth. Thus, *Tmprss6*^{-/-} newborn mice showed a 4.8-fold increase in expression levels of liver hepcidin in comparison to control mice (control: 485.7 ± 84.0 vs knock-out: 100.0 ± 25.1; *P* < 0.01; n=5 mice per genotype).

Because hepcidin is a negative regulator of iron export into plasma, we next explored the putative occurrence of iron deposits in the duodenum to evaluate if the anemic phenotype of *Tmprss6*^{-/-} mice could be due to a defective iron release into the circulation after diet absorption. Interestingly, Perls staining revealed notable cellular iron retention in duodenal enterocytes of *Tmprss6*^{-/-} mice (Figure 3E-F). Then, and considering that hepcidin blocks iron release through the down-regulation of ferroportin – the only known cellular iron exporter – we examined by immunohistochemistry the expression of this protein in the duodenum of wild-type and *Tmprss6*^{-/-} mice. As shown in Figure 3G, a marked positive staining was observed in the basolateral membrane of duodenal enterocytes of wild-type mice. By contrast, ferroportin expression was almost absent in the basal membrane of *Tmprss6*^{-/-} enterocytes (Figure 3H). Taken together, these results provide strong support to the hypothesis that the marked hepcidin up-regulation observed in *Tmprss6*^{-/-} mice leads to the subsequent ferroportin removal of the enterocytes from these animals, impairing iron export into plasma and finally leading to iron deficiency anemia in *Tmprss6*^{-/-} mice.

Iron therapy rescues alopecia and anemic phenotypes in *Tmprss6*^{-/-} mice

The above findings showing that iron deficiency anemia in *Tmprss6*^{-/-} mice was likely due to an impaired iron export into plasma, prompted us to consider the possibility of rescuing this phenotype by directly releasing iron into the circulatory system. Thus, *Tmprss6*^{-/-} adult mice received weekly an iron-dextran subcutaneous injection for a period of 4 weeks and the occurrence of putative changes in their

alopecia and hematological phenotypes was examined. As can be seen in Figure 4A, this iron-based therapy led to a complete recovery of hair in treated *knock-out* mice (Figure 4A). Likewise, this iron therapy rescued the hematological deficiencies observed in *Tmprss6*^{-/-} mice. Thus, blood smear examination revealed a marked reduction of hypochromic red cells in treated *Tmprss6*^{-/-} mice (Figure 4B). Finally, we evaluated if the initial hair loss phenotype observed in young *knock-out* mice was also iron-dependent. To this purpose we used a group of 10-day-old *Tmprss6*^{-/-} pups, which received weekly an iron-dextran subcutaneous injection for a period of 3 weeks. Consistent with the above findings in adult mice, this treatment completely prevented hair loss in all treated young animals (n=4, data not shown).

Discussion

A tightly regulated iron homeostasis is essential for life maintenance in eukaryotic organisms. Both, iron deficiency and iron overload cause severe pathologies in humans.²⁶ Stable plasma concentrations and adequate levels of cellular iron are maintained through the strict control of a series of critical steps that regulate its absorption, transport, storage and recycling. Over the last years, the use of loss- and gain-of-function animal models together with genetic studies in patients with inherited iron homeostasis disorders have allowed the identification of key genes involved in iron metabolism.^{27,28} Most of these genes are iron transporters specific of different cell types. However, our unexpected findings derived from the phenotype analysis of *Tmprss6*^{-/-} mice demonstrate for the first time that the lack of a proteolytic enzyme has severe consequences on iron balance under normal conditions. Thus, after generation and phenotype analysis of these mutant mice we first observed that *Tmprss6*-deficiency leads to severe iron deficiency anemia and hair loss. Further molecular analysis of tissues from the generated mutant mice revealed that matriptase-2 is required for the maintenance of normal hepcidin expression levels as assessed by the finding that *Tmprss6*^{-/-} mice showed significantly up-regulation in liver of the gene encoding this antimicrobial peptide. It is well established that hepcidin is a negative regulator of iron export which is primarily secreted by hepatocytes and acts as a circulating hormone.²⁹ Mice deficient in hepcidin and patients with mutations in this gene display a severe iron

overload disorder.^{30,31} Conversely, transgenic mice overexpressing hepcidin in liver develop severe iron deficiency anemia.³² Furthermore, it has been recently demonstrated that hepcidin controls iron levels through the binding to ferroportin, the major iron exporter into the plasma. Thus, hepcidin binding results in ferroportin internalization from the cell surface with the subsequent degradation in lysosomes.³³ It is also remarkable that conditional disruption of *ferroportin 1* gene causes iron deficiency anemia and iron accumulation in enterocytes.³⁴ Consistent with the marked up-regulation of hepcidin, mice deficient in matriptase-2 show both a dramatic decrease in ferroportin levels at the basal membrane of duodenal cells and a marked increase in iron deposits in these enterocytes. Furthermore, the rescue of the hematological phenotype after iron treatment of these mutant mice reinforces the hypothesis that the anemic phenotype observed in *Tmprss6*^{-/-} mice results from the blockade of intestinal iron export into plasma after dietary absorption.

Upstream regulators responsible for the control of hepcidin expression have become the focus of attention in recent years because of their importance in the understanding of anemia and iron overload pathologies. According to our results, matriptase-2 is a novel candidate to act as *in vivo* regulator of hepcidin levels and function. Hepcidin is mainly regulated at the transcriptional level in response to a number of processes that affect iron balance, such as defective erythropoiesis, anemia, hypoxia and inflammation.^{35,36} Bone morphogenic proteins (BMPs) are the main positive regulators of hepcidin transcription under normal conditions.³⁷ Binding of specific BMP ligands to BMP type I or type II receptors, located at the cell surface of hepatocytes, leads to an intracellular signalling cascade that results in phosphorylation of receptor-Smads (Smad1, Smad5 and Smad8) that complex Smad4 to activate hepcidin transcription. Interestingly, it has been recently described that hemojuvelin, a GPI-linked protein located at the cell surface of hepatocytes, acts as BMP co-receptor promoting hepcidin transcription.³⁷ However, soluble hemojuvelin released from the cell surface has been demonstrated to be a competitive antagonist of membrane-bound hemojuvelin, leading to a decrease in hepcidin transcription.^{38,39} In addition, it has been reported that the *in vitro* shedding of BMP receptors reduces Smad signalling activation in primary human bone cells.⁴⁰ These results suggest that proteolytic activity at the cell surface of hepatocytes might be considered as an important step in hepcidin regulation and iron balance. Nevertheless, further studies will be necessary to elucidate whether

matriptase-2 is the protease responsible for these proteolytic events presumably occurring at the pericellular space.

In conclusion, our results provide the first causal evidence that the absence of a protease has severe consequences on iron homeostasis under normal conditions. These findings are in agreement with the very recent results reported by Beutler's group describing an ENU mouse mutant in *Tmprss6* with a similar phenotype.⁴¹ Lack of matriptase-2 causes an iron deficiency anemia and a hair loss phenotype, characterized by hepcidin up-regulation and the blockade of intestinal iron export into plasma. Based on the results presented herein, we propose that matriptase-2-mediated functions constitute a novel step in hepcidin regulation. The recent finding that mutations in the human *TMPRSS6* gene cause iron-refractory iron deficiency anemia (IRIDA)⁴² turns *Tmprss6*^{-/-} mice into a useful genetic model for the analysis of molecular mechanisms that underlie human hematological disorders whose molecular basis is yet unclear.

Acknowledgements

We thank Drs. F.V. Alvarez, I. Santamaría, A. Gutiérrez-Fernández, J.M. Freije and A. Fueyo for helpful comments and advice, Dr. D.W. Melton for providing mouse ES cells, and M. Fernández, S. Alvarez, and M.S. Pitiot for excellent technical assistance. This work was supported by grants from FIS-Instituto Carlos III, Ministerio de Educación y Ciencia, Fundación Lilly, Fundación "M. Botín" and the European Union (FP7). The Instituto Universitario de Oncología is supported by Obra Social Cajastur-Asturias, Spain.

Authorship

Contribution: G.V. and C.L.O. designed the experimental work; A.R.F., F.M.L., A.M.P., C.G., F.R., A.A., T.B. and G.V. performed research; A.R.F., F.M.L., A.M.P., C.G., F.R., A.A., T.B., R.C., G.V. and C.L.O. analyzed data; and G.V., A.R.F. and C.L.O. wrote the paper.

Conflict of interest disclosure: The authors declare no competing financial interests.

References

1. Werb Z. ECM and cell surface proteolysis: regulating cellular ecology. *Cell*. 1997;91:439-442
2. Netzel-Arnett S, Hooper JD, Szabo R, Madison EL, Quigley JP, Bugge TH, Antalis TM. Membrane anchored serine proteases: a rapidly expanding group of cell surface proteolytic enzymes with potential roles in cancer. *Cancer Metastasis Rev*. 2003;22:237-258
3. Szabo R, Bugge TH. Type II transmembrane serine proteases in development and disease. *Int J Biochem Cell Biol*; 2007
4. Kitamoto Y, Yuan X, Wu Q, McCourt DW, Sadler JE. Enterokinase, the initiator of intestinal digestion, is a mosaic protease composed of a distinctive assortment of domains. *Proc Natl Acad Sci U S A*. 1994;91:7588-7592
5. Leytus SP, Loeb KR, Hagen FS, Kurachi K, Davie EW. A novel trypsin-like serine protease (hepsin) with a putative transmembrane domain expressed by human liver and hepatoma cells. *Biochemistry*. 1988;27:1067-1074
6. Dhanasekaran SM, Barrette TR, Ghosh D, Shah R, Varambally S, Kurachi K, Pienta KJ, Rubin MA, Chinnaiyan AM. Delineation of prognostic biomarkers in prostate cancer. *Nature*. 2001;412:822-826
7. Bugge TH, List K, Szabo R. Matriptase-dependent cell surface proteolysis in epithelial development and pathogenesis. *Front Biosci*. 2007;12:5060-5070
8. List K, Szabo R, Molinolo A, Sriuranpong V, Redeye V, Murdock T, Burke B, Nielsen BS, Gutkind JS, Bugge TH. Deregulated matriptase causes ras-independent multistage carcinogenesis and promotes ras-mediated malignant transformation. *Genes Dev*. 2005;19:1934-1950
9. List K, Haudenschild CC, Szabo R, Chen W, Wahl SM, Swaim W, Engelholm LH, Behrendt N, Bugge TH. Matriptase/MT-SP1 is required for postnatal survival, epidermal barrier function, hair follicle development, and thymic homeostasis. *Oncogene*. 2002;21:3765-3779
10. Chan JC, Knudson O, Wu F, Morser J, Dole WP, Wu Q. Hypertension in mice lacking the proatrial natriuretic peptide convertase corin. *Proc Natl Acad Sci U S A*. 2005;102:785-790
11. Lin B, Ferguson C, White JT, Wang S, Vessella R, True LD, Hood L, Nelson PS. Prostate-localized and androgen-regulated expression of the membrane-bound serine protease TMPRSS2. *Cancer Res*. 1999;59:4180-4184
12. Wallrapp C, Hahnel S, Muller-Pillasch F, Burghardt B, Iwamura T, Ruthenburger M, Lerch MM, Adler G, Gress TM. A novel transmembrane serine protease (TMPRSS3) overexpressed in pancreatic cancer. *Cancer Res*. 2000;60:2602-2606
13. Yamaguchi N, Okui A, Yamada T, Nakazato H, Mitsui S. Spinesin/TMPRSS5, a novel transmembrane serine protease, cloned from human spinal cord. *J Biol Chem*. 2002;277:6806-6812
14. Kim DR, Sharmin S, Inoue M, Kido H. Cloning and expression of novel mosaic serine proteases with and without a transmembrane domain from human lung. *Biochim Biophys Acta*. 2001;1518:204-209
15. Szabo R, Netzel-Arnett S, Hobson JP, Antalis TM, Bugge TH. Matriptase-3 is a novel phylogenetically preserved membrane-anchored serine protease with broad serpin reactivity. *Biochem J*. 2005;390:231-242
16. Cal S, Quesada V, Garabaya C, Lopez-Otin C. Polyserase-I, a human polyprotease with the ability to generate independent serine protease domains from a single translation product. *Proc Natl Acad Sci U S A*. 2003;100:9185-9190

17. Yamaoka K, Masuda K, Ogawa H, Takagi K, Umemoto N, Yasuoka S. Cloning and characterization of the cDNA for human airway trypsin-like protease. *J Biol Chem.* 1998;273:11895-11901
18. Hobson JP, Netzel-Arnett S, Szabo R, Rehault SM, Church FC, Strickland DK, Lawrence DA, Antalis TM, Bugge TH. Mouse DESC1 is located within a cluster of seven DESC1-like genes and encodes a type II transmembrane serine protease that forms serpin inhibitory complexes. *J Biol Chem.* 2004;279:46981-46994
19. Velasco G, Cal S, Quesada V, Sanchez LM, Lopez-Otin C. Matriptase-2, a membrane-bound mosaic serine proteinase predominantly expressed in human liver and showing degrading activity against extracellular matrix proteins. *J Biol Chem.* 2002;277:37637-37646
20. Ramsay AJ, Reid JC, Velasco G, Quigley JP, Hooper JD. The type II transmembrane serine protease matriptase-2--identification, structural features, enzymology, expression pattern and potential roles. *Front Biosci.* 2008;13:569-579
21. Parr C, Sanders AJ, Davies G, Martin T, Lane J, Mason MD, Mansel RE, Jiang WG. Matriptase-2 inhibits breast tumor growth and invasion and correlates with favorable prognosis for breast cancer patients. *Clin Cancer Res.* 2007;13:3568-3576
22. Lopez-Otin C, Overall CM. Protease degradomics: a new challenge for proteomics. *Nat Rev Mol Cell Biol.* 2002;3:509-519
23. Lopez-Otin C, Matrisian LM. Emerging roles of proteases in tumour suppression. *Nat Rev Cancer.* 2007;7:800-808
24. Hooper JD, Campagnolo L, Goodarzi G, Truong TN, Stuhlmann H, Quigley JP. Mouse matriptase-2: identification, characterization and comparative mRNA expression analysis with mouse hepsin in adult and embryonic tissues. *Biochem J.* 2003;373:689-702
25. Zheng B, Mills AA, Bradley A. A system for rapid generation of coat color-tagged knockouts and defined chromosomal rearrangements in mice. *Nucleic Acids Res.* 1999;27:2354-2360
26. De Domenico I, McVey Ward D, Kaplan J. Regulation of iron acquisition and storage: consequences for iron-linked disorders. *Nat Rev Mol Cell Biol.* 2008;9:72-81
27. Andrews NC. Iron homeostasis: insights from genetics and animal models. *Nat Rev Genet.* 2000;1:208-217
28. Schmidt PJ, Toran PT, Giannetti AM, Bjorkman PJ, Andrews NC. The transferrin receptor modulates hfe-dependent regulation of hepcidin expression. *Cell Metab.* 2008;7:205-214
29. Park CH, Valore EV, Waring AJ, Ganz T. Hepcidin, a urinary antimicrobial peptide synthesized in the liver. *J Biol Chem.* 2001;276:7806-7810
30. Nicolas G, Bennoun M, Devaux I, Beaumont C, Grandchamp B, Kahn A, Vaulont S. Lack of hepcidin gene expression and severe tissue iron overload in upstream stimulatory factor 2 (USF2) knockout mice. *Proc Natl Acad Sci U S A.* 2001;98:8780-8785
31. Weinstein DA, Roy CN, Fleming MD, Loda MF, Wolfsdorf JI, Andrews NC. Inappropriate expression of hepcidin is associated with iron refractory anemia: implications for the anemia of chronic disease. *Blood.* 2002;100:3776-3781
32. Nicolas G, Bennoun M, Porteu A, Mativet S, Beaumont C, Grandchamp B, Sirito M, Sawadogo M, Kahn A, Vaulont S. Severe iron deficiency anemia in transgenic mice expressing liver hepcidin. *Proc Natl Acad Sci U S A.* 2002;99:4596-4601

33. Nemeth E, Tuttle MS, Powelson J, Vaughn MB, Donovan A, Ward DM, Ganz T, Kaplan J. Heparin regulates cellular iron efflux by binding to ferroportin and inducing its internalization. *Science*. 2004;306:2090-2093
34. Donovan A, Lima CA, Pinkus JL, Pinkus GS, Zon LI, Robine S, Andrews NC. The iron exporter ferroportin/Slc40a1 is essential for iron homeostasis. *Cell Metab*. 2005;1:191-200
35. Nicolas G, Chauvet C, Viatte L, Danan JL, Bigard X, Devaux I, Beaumont C, Kahn A, Vaulont S. The gene encoding the iron regulatory peptide hepcidin is regulated by anemia, hypoxia, and inflammation. *J Clin Invest*. 2002;110:1037-1044
36. Tanno T, Bhanu NV, Oneal PA, Goh SH, Staker P, Lee YT, Moroney JW, Reed CH, Luban NL, Wang RH, Eling TE, Childs R, Ganz T, Leitman SF, Fucharoen S, Miller JL. High levels of GDF15 in thalassemia suppress expression of the iron regulatory protein hepcidin. *Nat Med*. 2007;13:1096-1101
37. Babitt JL, Huang FW, Wrighting DM, Xia Y, Sidis Y, Samad TA, Campagna JA, Chung RT, Schneyer AL, Woolf CJ, Andrews NC, Lin HY. Bone morphogenetic protein signaling by hemojuvelin regulates hepcidin expression. *Nat Genet*. 2006;38:531-539
38. Lin L, Goldberg YP, Ganz T. Competitive regulation of hepcidin mRNA by soluble and cell-associated hemojuvelin. *Blood*. 2005;106:2884-2889
39. Silvestri L, Pagani A, Camaschella C. Furin-mediated release of soluble hemojuvelin: a new link between hypoxia and iron homeostasis. *Blood*. 2008;111:924-931
40. Singhatanadgit W, Salih V, Olsen I. Shedding of a soluble form of BMP receptor-IB controls bone cell responses to BMP. *Bone*. 2006;39:1008-1017
41. Du X, She E, Gelbart T, Truksa J, Lee P, Xia Y, Khovananth K, Mudd S, Mann N, Moresco EM, Beutler E, Beutler B. The Serine Protease TMPRSS6 Is Required to Sense Iron Deficiency. *Science*. 2008
42. Finberg KE, Heeney MM, Campagna DR, Aydinok Y, Pearson HA, Hartman KR, Mayo MM, Samuel SM, Strouse JJ, Markianos K, Andrews NC, Fleming MD. Mutations in TMPRSS6 cause iron-refractory iron deficiency anemia (IRIDA). *Nat Genet*. 2008;40:569-571

Figure legends

Figure 1. Gene targeted disruption of the *Tmprss6* gene. (A) (Upper) Partial genomic structure of the murine *Tmprss6* gene. Exon coding sequences are indicated as black bars. (Lower) The targeting vector duplicates exons III to VI. E, *EcoRI*; S, *SspI*; N, *NdeI*; 3'*Hprt*, 3'-half *Hprt* minigene; *Puro*, puromycin resistance gene; Ag, *K14 Agouti* minigene. (B) Predicted structure of the targeted allele. (C) Southern blot analysis of DNA from *Tmprss6*^{+/+}, *Tmprss6*^{+/-} and *Tmprss6*^{-/-} mice digested with *SspI*. Hybridization with the 3'-external probe detects the expected 33 kb and 9 kb bands corresponding to wild-type and mutant alleles, respectively. (D) Northern blot analysis of liver tissues obtained from wild-type and *Tmprss6*^{-/-} mice showing the absence of full-length *Tmprss6* mRNA expression in mutant mice.

Figure 2. Alopecia phenotype in *Tmprss6*^{-/-} mice. (A) Representative photographs of 4-week-old *Tmprss6*^{+/+} and *Tmprss6*^{-/-} littermate mice. (B) Skin sections from 4-week-old wild-type and *Tmprss6*^{-/-} mice showing dystrophic hair follicles and hyperkeratosis in *Tmprss6*-null tissue, as compared with the wild-type. Bar represents 100 μ m, magnification 20X.

Figure 3. Heparin up-regulation reduces ferroportin expression and causes an anemic phenotype in *Tmprss6*^{-/-} mice. Wright-Giemsa-stained blood smears from *Tmprss6*^{+/+} (A) and *Tmprss6*^{-/-} (B) littermate mice. The figure shows the severe hypochromia found in mutant erythrocytes in comparison to wild-type ones. (C) Representative Northern blot analysis of liver tissues from wild-type and *Tmprss6*^{-/-} mice showing the increased hepcidin mRNA expression in mutant mice. (D) TaqMan real time PCR analysis of hepcidin expression in liver samples from 7-week-old *Tmprss6*^{+/+} and *Tmprss6*^{-/-} mice. mRNA levels on the y-axis are expressed relative to β -actin levels. The average relative expression of hepcidin in wild-type mice was assigned an arbitrary value of 100. Values are means \pm SEM. **P* < 0.05; n=5 mice per group. Perl's Prussian blue stain for iron in sections of duodenal villi of 5-week-old *Tmprss6*^{+/+} (E) and *Tmprss6*^{-/-} mice (F) shows iron accumulation in *Tmprss6*-null enterocytes. Representative immunostaining of ferroportin in duodenal tissue from 5-week-old *Tmprss6*^{+/+} (G) and *Tmprss6*^{-/-} mice (H). Arrow points the basal expression of ferroportin in wild-type enterocytes whereas positive basal staining is absent in

Tmprss6-null cells. Bars represent 10 μ m, magnification 100X (A-B) and 20 μ m, magnification 60X (E-H).

Figure 4. Iron-dextran therapy rescues the *Tmprss6*^{-/-} phenotype. (A) Representative photograph of a 2-month-old *Tmprss6*^{-/-} mice before (Left) and after one month iron-dextran treatment (Right). (B) Wright-Giemsa-stained blood smears from untreated (Top) and iron-dextran injected (Bottom) *Tmprss6*^{-/-} mice. Bar represents 10 μ m, magnification 100X.

Table 1. Reduced plasma iron and transferrin saturation in *Tmprss6*^{-/-} mice.

	Plasma iron (μ g/dL)	UIBC (μ g/dL)	Tf saturation (%)
<i>Tmprss6</i> ^{+/+}	113.3 \pm 6.6	237.5 \pm 41.5	34.1 \pm 3.5
<i>Tmprss6</i> ^{-/-}	***47.9 \pm 5.8	*375.2 \pm 14.6	***11.3 \pm 1.3

Plasma iron content, unsaturated iron binding capacity (UIBC) and transferrin (Tf) saturation were determined in 6-week-old wild-type and *Tmprss6*^{-/-} mice. Data are shown as mean \pm SEM. ****P* < 0.001, **P* < 0.05, n=6 mice per group.

Table 2. Red blood cell parameters of *Tmprss6*^{-/-} mice.

	Hgb (g/dL)	Hct (%)	MCV (fL)	MCH (pg)	MCHC (g/dL)
<i>Tmprss6</i> ^{+/+}	16.4 \pm 0.3	51.5 \pm 1.1	49.8 \pm 0.9	15.8 \pm 0.2	31.8 \pm 0.6
<i>Tmprss6</i> ^{-/-}	***12.0 \pm 0.5	*44.3 \pm 1.9	***37.5 \pm 0.4	***10.2 \pm 0.2	**27.1 \pm 0.8

Hemoglobin (Hgb), hematocrit (Hct), mean cell volume (MCV), mean cell hemoglobin and mean cell hemoglobin concentration (MCHC) were determined in 8-week-old wild-type (n=5) and *Tmprss6*^{-/-} (n=4) mice. Data are shown as mean \pm SEM. ****P* < 0.001, ***P* < 0.01, **P* < 0.05.

Figure 1

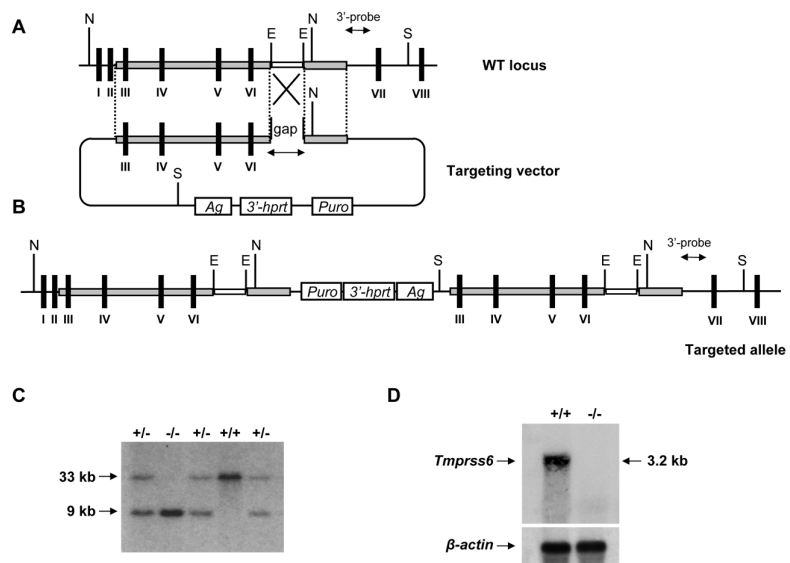


Figure 2

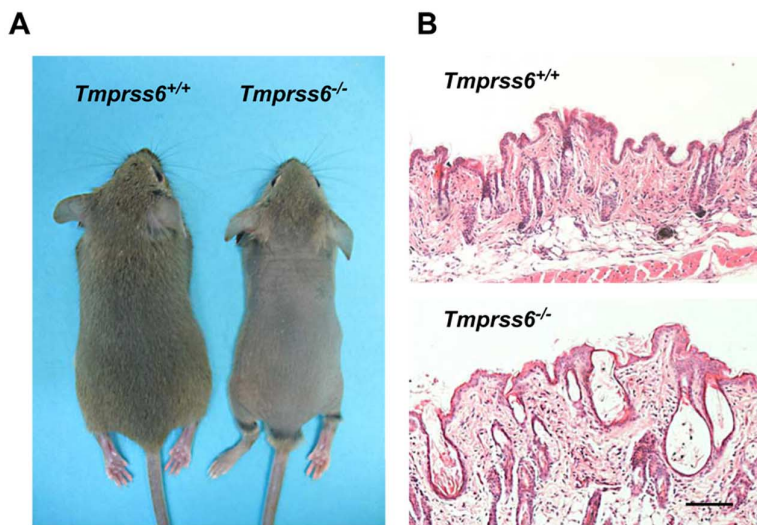


Figure 3

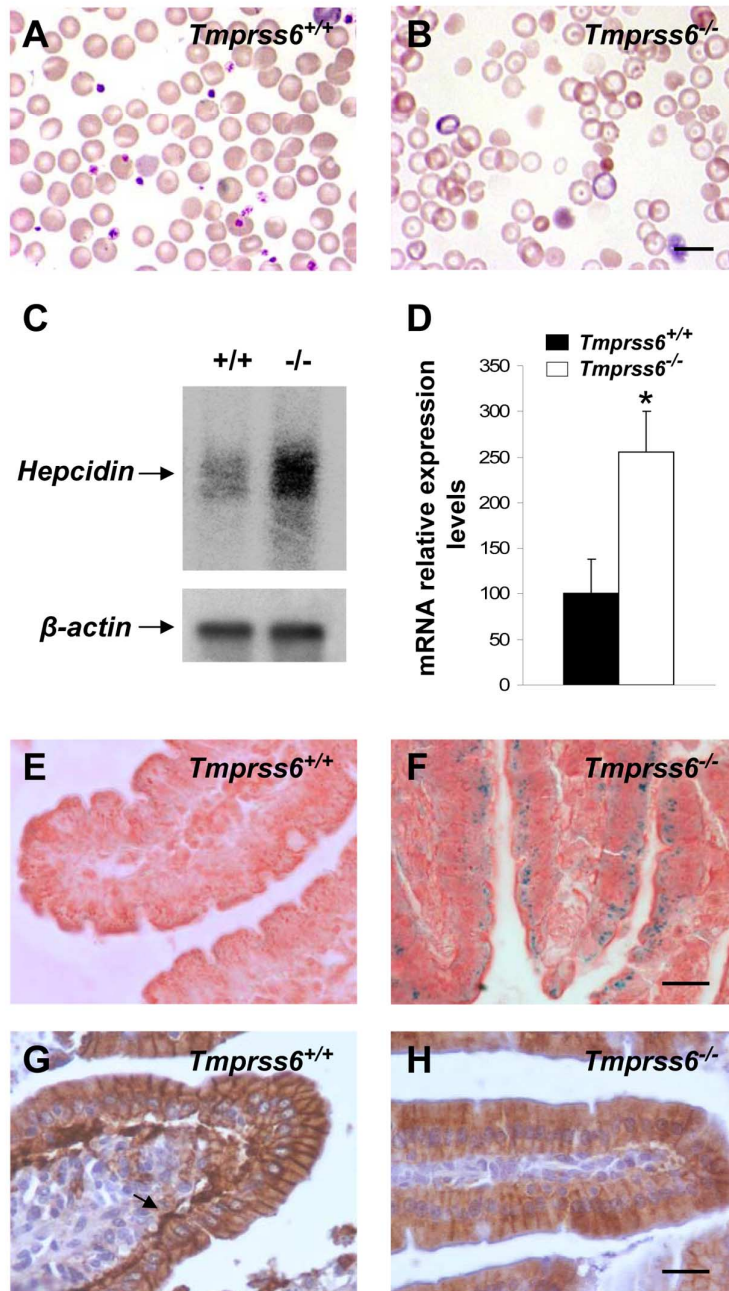


Figure 4

